Union College
Union | Digital Works

Honors Theses   Student Work

6-2014

Application of a High-Performance Optically Enhanced Solar Thermal Collector System

Timothy H. Cameron
Union College - Schenectady, NY

Application of a High Performance-
Optically Enhanced Solar Thermal Collector System

By

Timothy H. Cameron

****

Submitted in partial fulfillment
of the requirements for
Honors in the Department of Mechanical Engineering

UNION COLLEGE
June, 2014

ABSTRACT

CAMERON, TIMOTHY H   Application of a High Performance-Optically Enhanced Solar Thermal Collector System. Department of Mechanical Engineering, June 2014.

ADVISOR: Richard D. Wilk

In an effort to make Union College a more environmentally friendly campus, this research project focuses on the application of Union's liquid-based solar thermal collector system. The motivation for this research project is due to the increasing demand for renewable energy sources in order to decrease our society's dependence on fossil fuels. The system features nine, 16-tube, evacuated tube solar modules which absorb radiant solar energy from the sun. Through a two loop system, thermal energy is stored in water within two-80 gallon storage tanks. This research project involves the design, construction, and analysis of two applications in order to utilize the systems 80 MJ of daily thermal output. The two applications constructed are for both air and water heating purposes. The first application involves a liquid-air heat exchanger which is used to provide space heating. The second application involves a liquid-liquid heat exchanger, creating a boiler water pre-heat system. By utilizing the availability of solar energy, these applications will decrease Union College's carbon footprint.

CONTENTS

List of Figures

List of Tables

1. Introduction

The motivation for this research project was due to the increasing demand for renewable energy sources in order to decrease our society's dependence on fossil fuels. Our generation is faced with the growing concern of global warming and its impact on the environment, as well as the depletion of the world's non-renewable fossil fuels.

The main cause of global warming can be contributed to carbon dioxide being released in to the atmosphere due to the burning of fossil fuels. Carbon dioxide accounts for 84% of all greenhouse gas emissions as a result of human activates [1]. The increase of greenhouse gas emissions over the past century has led to an average global temperature increase of 1.4 ^{o}F, which is the precursor for a variety of environmental concerns [2].

In an effort to make Union College a more environmentally friendly campus, the New York State Energy Research Development Authority (NYSERDA) sponsored Union College in a research project to construct a solar-thermal collector system. The NYSERDA has a mission to "facilitate change through the widespread development and use of innovation technologies to improve the State's energy, economic, and environmental wellbeing [3]." Its sponsorship at Union College aimed to demonstrate the efficiency of a liquid-based solar heating system in order to provide thermal energy for a variety of applications.

The existing system at Union College consists of two loops; a solar thermal and a thermal fluid transport and storage system. The solar thermal loop consists of nine, 16-tube,

evacuated tube solar modules. The loop consists of a 50/50 propylene glycol-water solution as the working fluid in order to perform in the low winter temperatures. This loop is connected to the thermal fluid storage and transport loop through a flat plate heat exchanger. The storage loop consists of two, 80 gallon water storage tanks. Under ideal conditions, the system was able to produce energy at a rate of 13 kW and a total thermal output of 80 MJ [4].

The goal of this project was to apply the existing solar thermal system with different loading applications to utilize the vast amount of energy that the system produces. The following report will discuss the preliminary research done to understand its function as well as potential designs for applications for the system. A long-term study on the Facility Building's hot water-consumption was conducted in order to determine if there was possible motivation to use the solar system to heat this water in the hot water heater. In conjunction with that study, a heat transfer analysis of the existing flat plat heat exchanger was conducted in order to determine the amount of heat transferred because a similar heat exchanger would be used for this application. A flat plate heat exchanger was purchased and a small scale circulation loop was constructed in the laboratory in order to characterize the heat exchanger as well as simulate the concept. A characterization of a liquid-air heat exchanger was also conducted because it could provide space-heating, which is another possible application.

Overall, the main objective of this report is to discuss preliminary research undertaken to further enhance the solar thermal collector system located at Union College.

2. Background and Literature Survey

Solar thermal energy is obtained by harnesses radiant solar from the sun and storing it as thermal energy, or heat, in a liquid working fluid. Solar thermal collector systems can either be made for residential of commercial applications depending on energy demands. Residential solar thermal collector systems are used in a variety of applications including swimming pool heating and storage tank heating for use in showers, washing machines and dishwashers. Commercial systems, where the energy demands are greater, are also generally used for hot water applications [5]. Although heating applications are the most common use for these types of systems, solar cooling through an absorption chiller is also a potential application. There are a variety of different types of solar collectors that can be used including flat plate and evacuated tube solar collectors.

The most common type of residential hot water systems use flat plate solar collectors (Figure 1) due its easy installation upon slanted rooftops and minimal amount of assembly components. The flat plate collector consists of a dark flat plate absorber, usually made of silicon, within a transparent glass cover. Copper piping runs the length of the panel, circulating the working fluid, which is usually water or a glycol mixture. The collector works by absorbing radiant solar energy on the black panel which is then trapped within the glass cover due to the greenhouse effect. The thermal energy is then transferred to the working fluid, which can then be stored within a storage tank [6].

Figure 1: Flat plate solar collector. [6]

Evacuated tube solar collectors are more commonly used in commercial applications. The evacuated tube moduli come in a variety of types including; flat absorber heat pipes (Figure 2 top), curved absorber heat pipes (Figure 2 bottom), and flat absorber heat pipes with flow through [4]. The evacuated tube modulus consists of a glass cylindrical shell with the same type of dark, flat plate absorber as in the flat plate design. The glass tube is under a vacuum which greatly reduces the amount of convection and conduction leading to heat loss. This results in a higher efficiency than the flat plate model. Moduli with flat absorber heat pipes and curved absorber heat pipes have similar efficiency but configuration depends on the manufacturer. These types of collectors contain a closed copper heat tube along the absorber, containing an alcohol mixture. As the copper heat tube absorbs solar energy, it transfers it to a circulating working fluid within its manifold. The difference between these types of absorbers and a flow through absorber is that the working fluid circulates through the actual moduli of the flow through instead of just the manifold [7].

Figure 2: Flat absorber evacuated tube heat pipe (top). Curved Pipe evacuated tube heat pipe (bottom). [4]

The choice of which type of solar thermal moduli to use depends on the desired

application.

3. Design Description

The objective of the project is to design and test a mulit-system load loop to the existing solar-thermal system atop the Facilities Building at Union College in order to utilize the solar thermal energy that it produces. The approach that was taken to facilitate this task was first to investigate and then design these applications. Both applications that being considered are for heating purposes, both for water and air heating. These applications include: Application 1: Liquid-Air Heat Exchanger, and Application 2: Boiler Water Preheat System.

3.1 Existing Solar Thermal Collector System

A schematic of the existing solar thermal system is displayed in Figure 3.
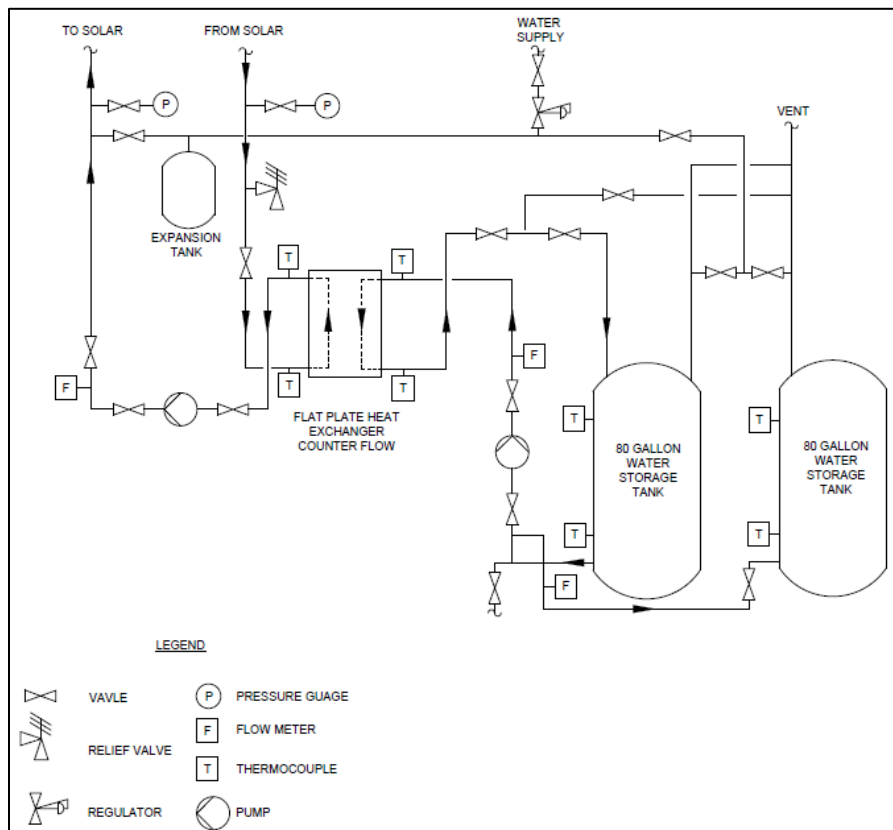
Figure 3: Schematic of the existing solar thermal collector system.

Both Applications will be utilizing the thermal energy from the water stored within the two 80-gallon storage tanks. Both applications will tap off of the left storage tank. The one supply port on the tank will split, allowing for both applications to be operated individually or simultaneously.

3.2 Application 1: Liquid-Air Heat Exchanger

A schematic of Application 1 is displayed in Figure 4. This application features a circulating loop between the water storage tank and the liquid-air heat exchanger which will provide space heating to the Facilities Building. Water will be pumped from the supply port of the storage tank, through the heat exchanger, and back to the storage tank. The thermal energy from the water will be transferred to the air using six axial fans located on the front face of the heat exchanger.
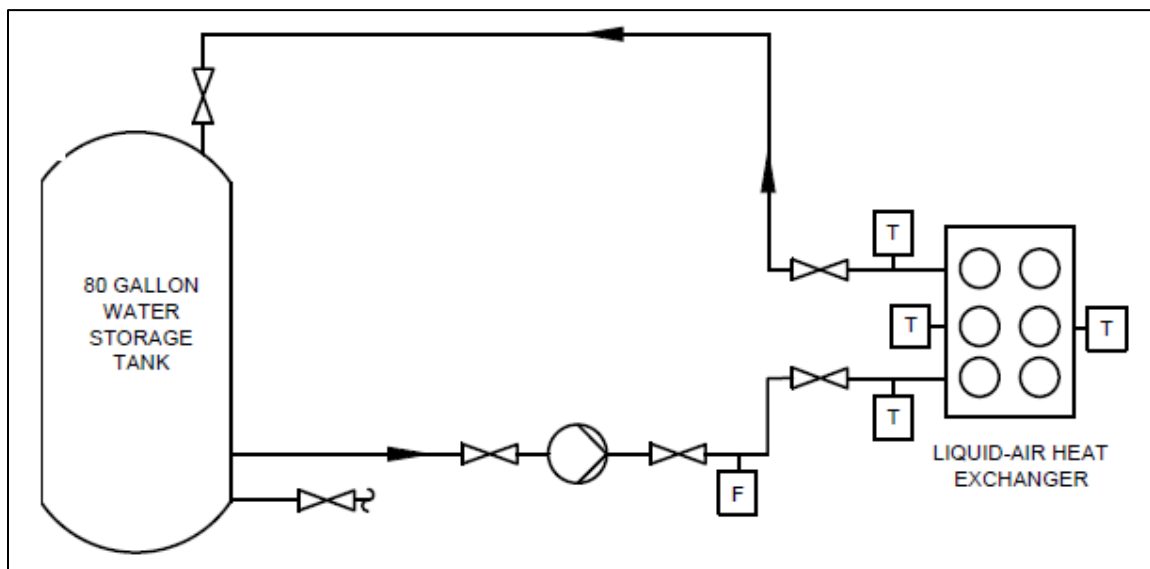
Figure 4: Schematic of Application 1: Liquid- Air Heat Exchanger.

Copper piping will be used for this application. Manual level-ball valves will be placed before and after the pump and heat exchanger for safety and maintenance purposes. An

in-line bronze centrifugal pump will be used to prevent corrosion because the loop and storage tank are vented at atmospheric pressure. An in-line flow meter will be placed upstream of the pump to measure the flow rate. On the water side, tee type pipe fittings will be placed at the inlet and outlet of the heat exchanger to insert thermocouple probes to measure water temperatures. Type K thermocouples will also be placed on the air inlet and outlet sides of the heat exchanger.

3.3 Application 2: Boiler Water Preheat System

A schematic of Application 2 is displayed in Figure 5. This application will feature a circulating loop between the water storage tank and a counter-flow, flat plate, liquid-liquid heat exchanger. The other side of the heat exchanger will tap into the municipal water supply before entering the natural-gas boiler. The flat plate heat exchanger will transfer thermal energy from the storage loop to the municipal water, which will heat the water before entering the boiler.
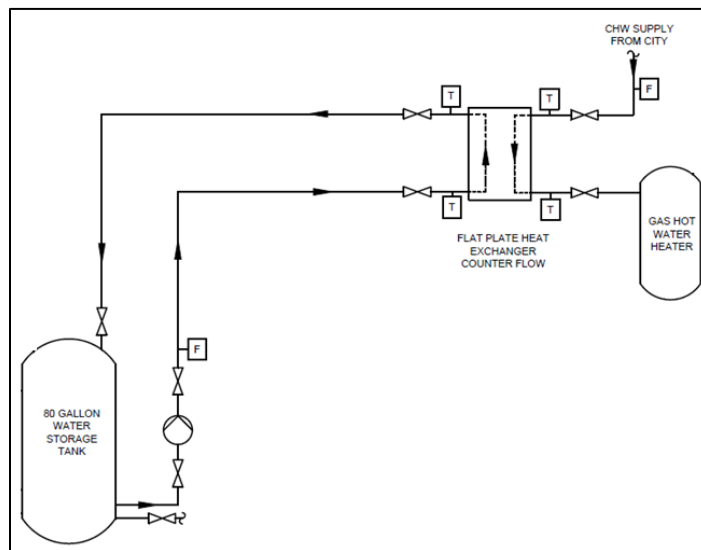
Figure 5: Schematic of Application 2: Boiler Water Preheat System.

Most of the same features in Application 1 will also be provided in Application 2. Copper piping will be used along with manual level-ball valves before and after the pump and on all four inlets to the heat exchanger. An in-line bronze centrifugal pump will be used along with an in-line flow meter to measure flow rate on circulating loop. A cumulative flow meter has already been placed on the municipal water supply to measure water consumption. Type K thermocouple probes will be placed on all four inlets to the heat exchanger.

4. Analysis

4.1 Application 1: Description of Heat Exchanger

The heat exchanger being used in this application was donated to Union College and therefore the specifications of the heat exchanger were unknown. All that is known is that its manufacturer was Super Radiated Coils.

The type of heat exchanger is an air to liquid cross-flow heat exchanger, with staggered coils. This type of heat exchanger is able to transfer thermal energy by flowing fluids perpendicular to each other; the liquid passes through parallel tubes and the air passes across them. A schematic of this setup is displayed in Figure 6.
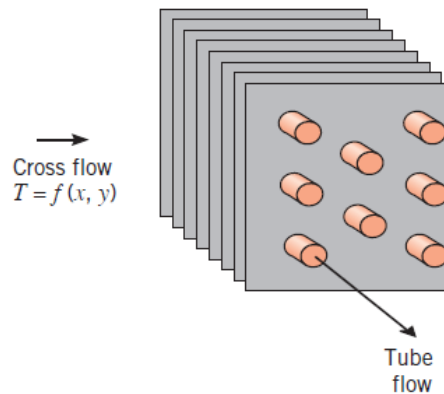
Figure 6: Cross-Flow Heat Exchanger with staggered coils. [8]

The actual heat exchanger used is displayed in Figure 7. The left view displays the staggered coil arrangement. The right view displays the supply and return header on the liquid side into the coils. The rear view displays the cross-flow arrangement, where the air enters directly into the heat exchanger. The front view displays the six fans that draw air through the heat exchanger.

The dimensions of the heat exchanger are displayed in Table I. On the liquid side, water flows into the supply header of the heat exchanger and then into 13 tubes, which then form 6 coil layers deep before exiting through the return header. The approximate outside diameter (OD) of the tubes is 9.8 mm. On the air side, air flows into the rear of the heat exchanger parallel to the fins which are spaced 500 fins/meter, for a total of 250 fins. The total face area is 0.2 m^2. The heat exchanger is a mixed-unmixed, where the air is mixed and the water is unmixed.
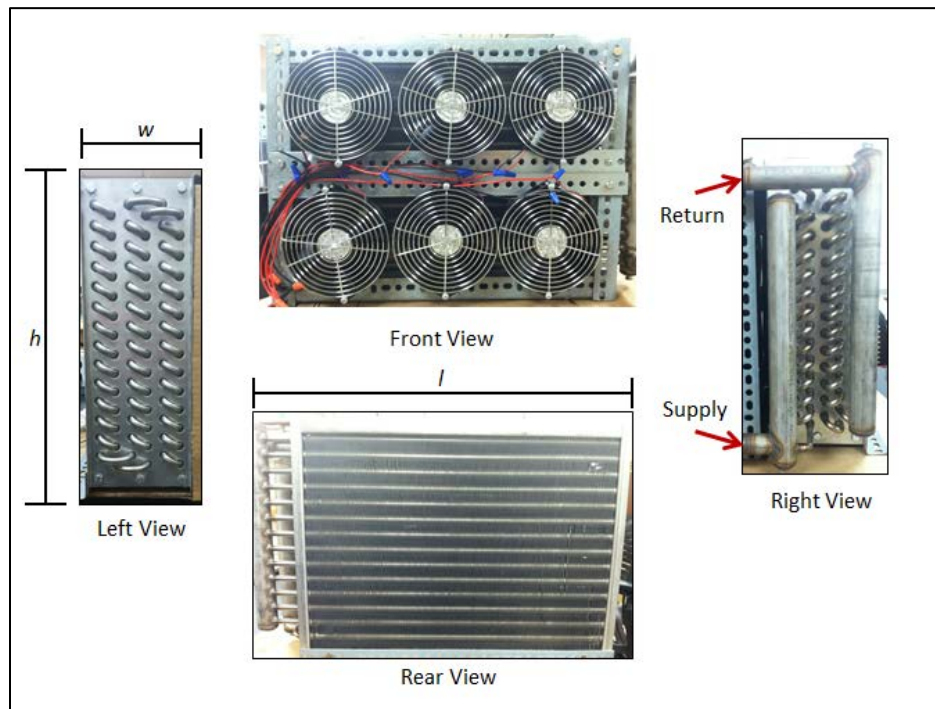
Figure 7: Different views of liquid-air heat exchanger.

Dimensions of Heat Exchanger		
l (cm)	Length	50
w (cm)	Width	14
h (cm)	Height	40
NR	# of tube layers high	13
NC	# of tube layers deep	6
NF (#fins/meter)	# of fins per meter	500

Located on the front face of the heat exchanger there are six, ebm-papst type 7112 N fans (Figure 8). Each fan is powered by 12 DC volts. The six fans are used to draw air through the heat exchanger.
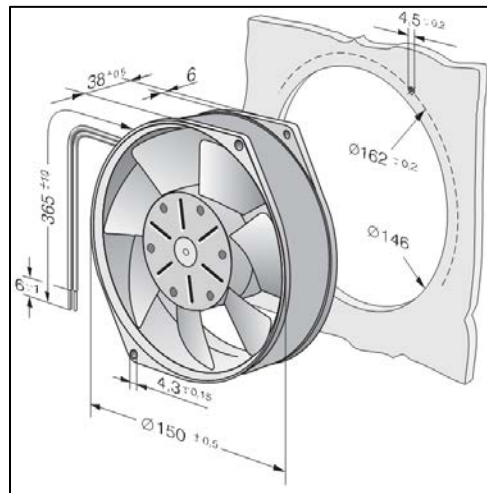
Figure 8: Schematic of ebm-papst type 7112 N fans. [9]

4.2 Application 1: Testing Equipment and Procedure

Before the selected heat exchanger could be installed into the solar-thermal system in the Facilities Building, it was first characterized to determine its thermal capabilities. The following is a description of the equipment and setup used to perform this study. A picture of the testing apparatus is displayed in Figure 9.
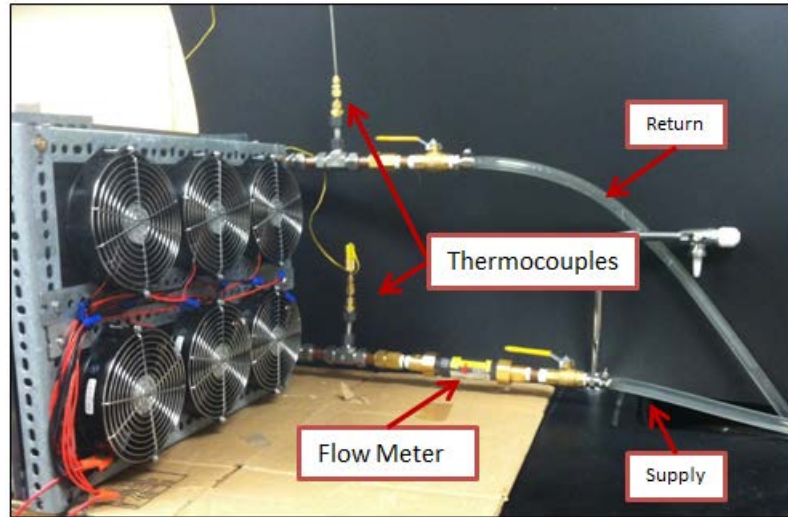
Figure 9: Heat exchanger testing apparatus.

Hot water was supplied to the heat exchanger from the sink faucet using the municipal water supply. Its flow rate and temperature could be altered by adjusting the knobs while the flow rate was measured using a Hedland EZ-VIEW flow meter. Water-resistant clear polyurethane tubing (1/2") was used to supply and return the water to the drain.

Ambient Air was supplied to the heat exchanger using the fans previously discussed. A Summit Company LTD. SRP- 3003D was used to supply DV voltage. The fans operated at 12 DCV and 1 Amp. A Prova Instruments Ins. flow anemometer AVM-07 was used to measure the air velocity and air volumetric flow rate.

The inlet and the outlet temperatures for the water were measured using type K thermocouple probes while the temperature of the air was also measured using type K thermocouples. The values were recorded using a Measurement Computing iotech Personal Data Acquisition System/45 (DAQ).

4.3 Application 1: Characterization of Heat Exchanger

In order to determine the overall effectiveness of the heat exchanger, multiple trials were conducted and temperature and flow rate data was recorded. The heat rate transferred (q) on both the water and the air side was calculated using Equation (1).

$$q = \dot{m} c_p (T_h - T_c) \tag{1}$$

where　　　　$\dot{m}$ = mass flow rate of fluid

　　　　　　c_p = specific heat of fluid

　　　　　　T_h = hot temperature of fluid

　　　　　　T_c = cold temperature of fluid

Since the specific heat and the density of a fluid (ρ) are temperature dependent, the values were taken at an average of the inlet and outlet state. The mass flow rates of fluids were calculated using the measured volumetric flow rate ($\dot{V}$), as displayed in Equation (2).

$$\dot{m} = \dot{V} \rho \tag{2}$$

The fluid properties used in these calculations are displayed in Table II.

Table II: Fluid properties of both water and air. [10]

	Water (@ 45 °C)	Air (@ 30 °C)
ρ (kg/m³)	990.2	1.165
c_p (kJ/kgK)	4.181	1.005

Each trial was conducted over twenty minutes to account for any transient responses in the temperature readings. Figure 10 displays the transient responses of the water and air through the heat exchanger for trail 1. All temperatures display a large initial spike and then level out due to the heat loss through the heat exchanger itself, copper piping, and tubing. The temperatures approach equilibrium quickly and then remain relatively constant over the duration of the trail.
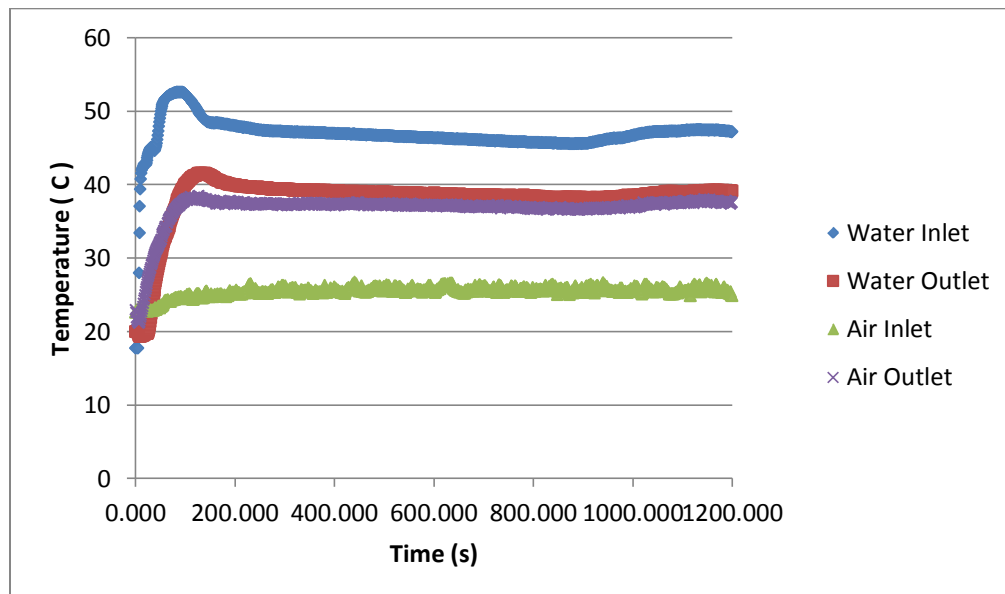
Figure 10: Transient responses of both the air and water through the heat exchanger for Trial 1.

For trail 1, Figure 11 displays the final steady state temperatures. The mass flow rates of each fluid are given. The volumetric flow rate of water for this trail was 2 gpm. The temperature difference was calculated to be 8.1 $^{\circ}$C on the water side and 12.1 $^{\circ}$C on the air side. The heat rate on the water side was calculated to be 4.3 kW while the heat rate on the air side was calculated to be 3.1 kW. The 28% difference in heat rates can be contributed to heat loss through the heat exchanger due to lack of insulation.
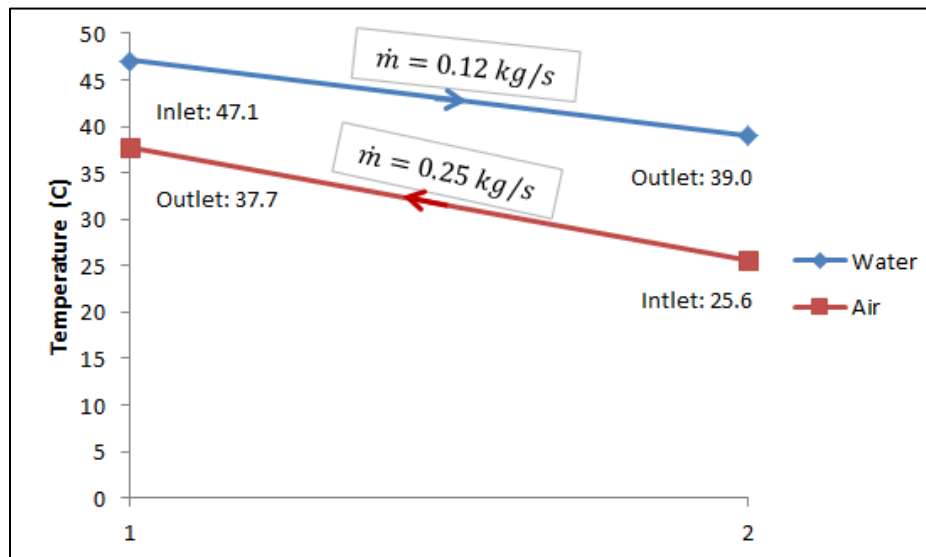
Figure 11: Plot of the inlet and outlet heat exchanger temperatures for both the air and water.

Trial 2 was conducting with the same air flow rate but an increased water flow rate of 2.5 gpm. Figure 12 displays the final steady state temperatures of trial 2.
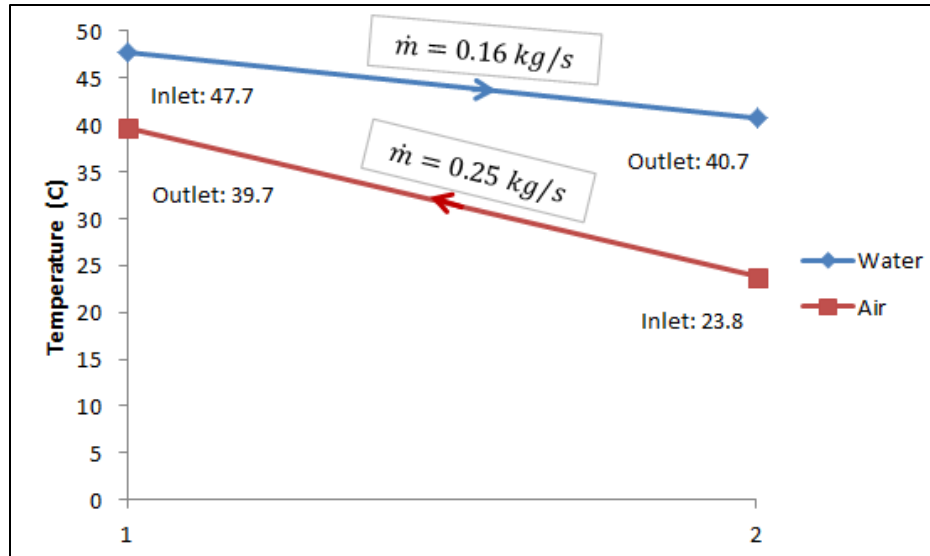
Figure 12: Plot of the inlet and outlet heat exchanger temperatures for both air and water.

The heat rate on the water side was calculated to be 4.6 kW while the heat rate on the air side was calculated to be 4.0 kW. As predicted, increasing the mass flow rate of the fluid also increased the amount of heat transferred between the fluids. There was only a 12% difference in the heat rates. The temperature difference was calculated to be 7.0 $^{\circ}$C on the water side and 15.9 $^{\circ}$C on the air side.

The testing apparatus and procedure provided limitations on the testing conditions of the heat exchanger. The municipal water supply limited the maximum inlet water temperature to approximately 48 $^{\circ}$C and flow rate to 2.5 gpm. Research has shown that the storage tank water temperatures can approach 90 $^{\circ}$C.

The overall heat transfer coefficient-surface area product (*UA*) was calculated using both the Log Mean Temperature Difference (*LMTD*) method and the Effectiveness-NTU method. First the *LMTD* method was used to calculate *UA* using Equation (3).

17

$$q = F * UA * \Delta T_{LM} \tag{3}$$

where   F = correction factor for cross-flow heat exchangers

ΔT_{LM}= log mean temperature difference

Due to the geometry of cross-flow heat exchangers, the *LMTD* is not always an accurate representation of the temperature difference. Therefore a correction factor (*F*) should be applied to the analysis. The calculations for *UA* are displayed in Table III using the air side heat rate and an assumed correction factor of 1.

<center>Table III: UA value for the heat exchanger using LMTD method.</center>

	Trial 1	Trail 2
Q (kW)	3.1	4.0
LMTD	10.0	10.8
UA (W/°C)	**307**	**370**

The Effectiveness-NTU method was used to calculate UA by first calculating the effectiveness (ε), as displayed in Equation (4).

$$\varepsilon = \frac{q}{q_{max}} = \frac{q}{C_{min}(T_{w,i}-T_{a,i})} \tag{4}$$

where q_{max} = maximum possible heat transfer

C_{min} = minimum product of $\dot{m}c_p$ of the two fluids

The number of transfer units (NTU) was then calculated using Equation (5) for a single pass, cross-flow heat exchanger with C_{min} mixed and C_{max} unmixed [8].

$$NTU = -\left(\frac{1}{C_r}\right)\ln[C_r\, ln(1 - \varepsilon) + 1] \tag{5}$$

where $\qquad C_r = C_{min}/C_{max}$

The UA value was then calculated using Equation (6). The values associated with this computation are displayed in Table IV.

$$NTU = \frac{UA}{C_{min}} \qquad\qquad (6)$$

Table IV: UA value for the heat exchanger using the ε-NTU method.

effectiveness (ε)	0.67
NTU	1.4
UA (W/°C)	**551**

The difference in *UA* values using the *LMTD* and the ε-*NTU* method could be a result of the assumed value of 1 for the correction factor (*F*) in the *LMTD* method. In actuality this number would be less than 1, resulting in a greater *UA* value.

The power consumption of each of the fans was calculated given the DC voltage and current used to power them. The total power needed to run the fans was 72 W; the corresponding calculation is displayed in Table V. The fans operate at a speed of 2850 1/s.

Table V: Displays the energy consumption of the fans.

Voltage (DCV) per fan	12
Current (A) per fan	1
Power (W) per fan	12
Total Power (W)	**72**

The measured volumetric flow rate through each fan was then used to determine its corresponding pressure drop. Given the fan specifications from the manufacture, the fan performance map (Figure 13) was used to estimate the pressure drop at the specified power.
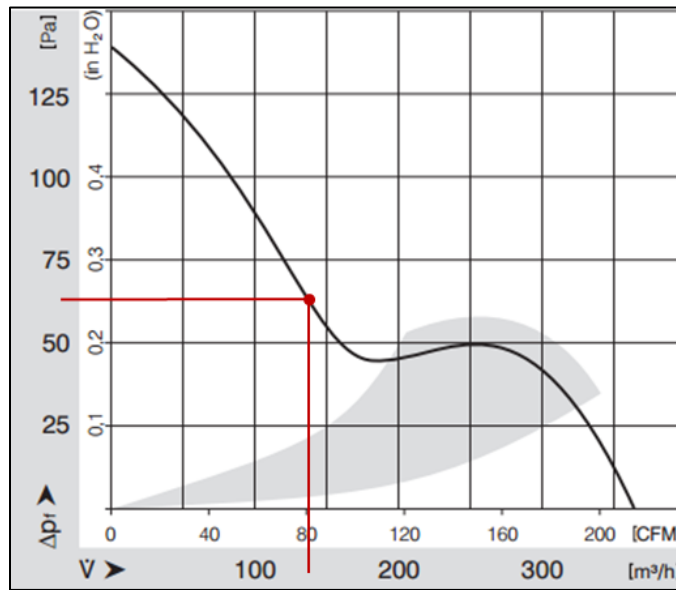
Figure 13: Performance map of the 7112 N DC axial compact fans. [9]

The volumetric flow rate of 130 m^3/hr through each fan corresponds to a pressure drop of approximately 65 Pa. The pressure drop is a result of the flow through the heat exchanger. It is estimated that the total pressure drop through the air side of the heat exchanger is 390 Pa.

4.4 Application 2: Evaluation of Facilities Building Water Consumption

In order to determine if the installation of a boiler pre-heat system was a practical application for the Facilities Building, the hot water consumption was monitored over a 24 week time period. An iSTEC 1700 Series Water Meter (Figure 14) was installed on the municipal water supply to measure the cumulative chilled water supplied to the boiler.

Figure 14: iSTEC 1700 Series Water Meter installed on the boiler water supply.

Figure 15 display the cumulative water consumption as well as the weekly water consumption over the time period. The average weekly Schenectady weather temperatures were also recorded to see if there was a correlation between the colder winter temperatures and the water consumption. A complete list of the temperature data is displayed in Appendix A.
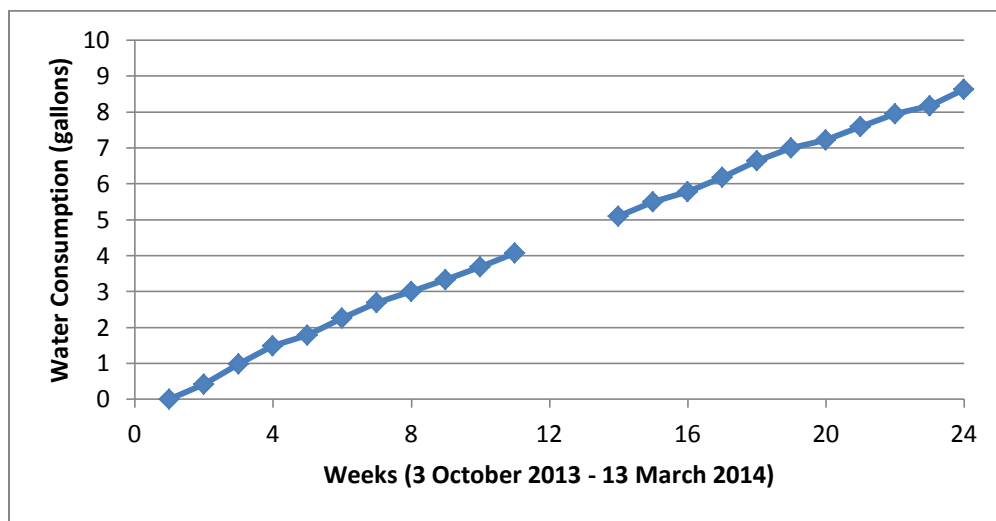
Figure 15: Plot of the cumulative hot water consumption of the Facilities Building.

Over the 24 week period, the facility only consumed 8.638 gallons of water. The usage displayed a fairly linear trend. There was no strong correlation between the decreasing winter temperatures and water consumption.

4.5 Application 2: Analysis of Existing Flat Plate Heat Exchanger

An analysis of the existing flat plate heat exchanger of the solar thermal system was conducted to analyze its thermal capabilities. The flat plate heat exchanger connects the solar loop and the thermal fluid storage loop. The type of heat exchanger is a counter-flow, space saving, high efficiency, flat plate heat exchanger (Figure 16). Its surface area is 6.9 ft^2, and has a maximum flow capacity of 14 gpm [10].

Figure 16: Existing flat plate heat exchanger in the solar thermal system.

The temperatures and flow rates through the heat exchanger were analyzed over a two day time period. Temperatures were measured using thermocouple type K probes and flow rates were measured using Hedland EZ-VIEW flow meters. The heat rate on both the solar loop and the storage loop were calculated. The water properties used in the

calculations were taken at an average temperature of 50 $^{\circ}$C. These properties are displayed in Table VI.

Table VI: Water properties used in the analysis of the flat plate heat exchanger.

	Solar Loop	Storage Loop
$\dot{V}$ (gpm)	2	2
$\dot{m}$ (kg/s)	0.12	0.12
c_p (kJ/kgK)	4.182	4.182

Figure 17 displays a plot of the heat rates of the flat plate heat exchanger on both the solar loop and the storage loop.
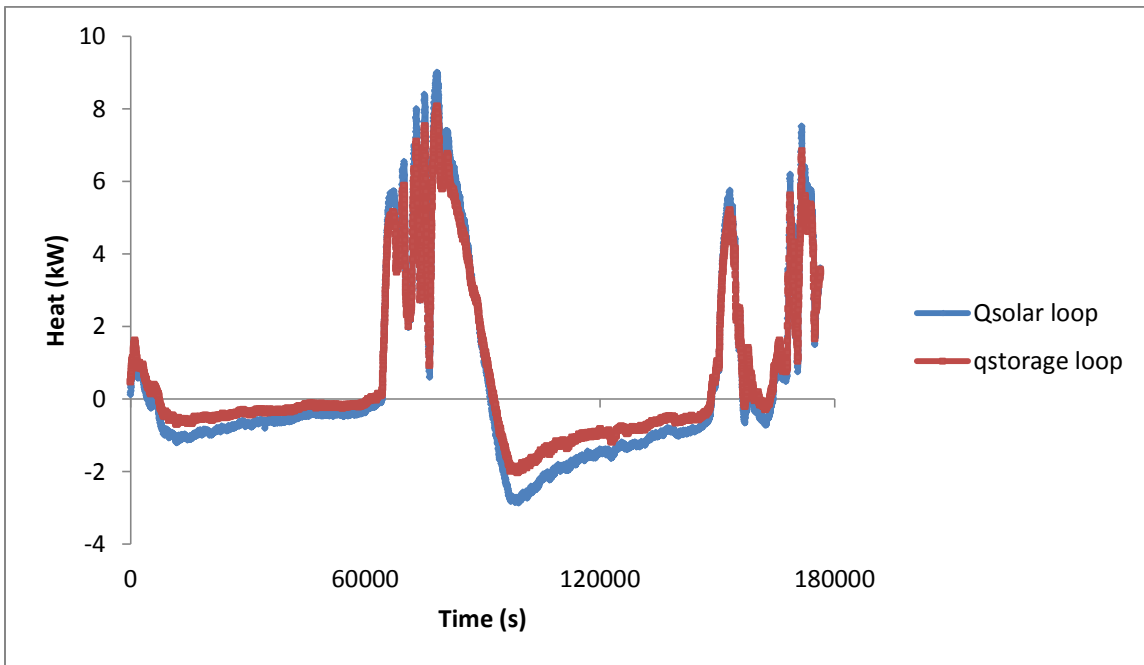
Figure 17: Heat rates on both the solar loop and the storage loop of the flat plate heat exchanger.

The maximum heat transferred on the solar loop side was 9.0 kW. Considering the maximum cooling capacity of the heat exchanger is approximately 45 kW, the heat exchanger is being underutilized. This is due to limitations of the system in that the flow

23

being provided to the heat exchanger on both sides is at 2 gpm, which is well under its 14 gpm maximum.

During testing, there is uncertainty in the measurements. Uncertainty in the flow rates can be contributed to the flow meter display as well as human error. A flow rate error was approximated to be 20% and was taken account in this analysis. There is also uncertainty associated with the temperatures measurements contributed by the thermocouples.

4.6 System Modelings

A system model was developed to model the storage water temperatures in the two 80 storage tanks over time. When the system is running, thermal energy will be supplied to the tank from the solar system, while thermal energy is also being drawn from the system by the loads as well as due to heat loss. The storage water temperature is an indicator of the net energy draw from the storage tank and the amount of heat being transferred in and out. An energy balance on the storage tank is expressed in Equation (7) [4].

$$mc_p \frac{dT_s}{dt} = Q_{solar} - Q_{Load} - Q_{TankLoss} \qquad (7)$$

where   m = mass of thermal storage (water)

T_s = water storage tank temperature

t = time

c_p = specific heat of thermal storage (water)

Q_{solar} = rate of heat delivered to tank from solar system

Q_{Load} = rate of heat out of tank to supply load

$Q_{TankLoss}$ = rate of heat loss from the thermal storage tank

The rate of heat loss from the thermal storage tank is expressed in Equation (8).

$$Q_{TankLoss} = (UA)_s(T_s - T_a) \qquad (8)$$

where $(UA)_s$ = storage overall heat loss coefficient – surface area product

T_a = storage tank ambient air temperature

Through numerical integration of Equation (7), a time dependent function for T_s is derived and displayed in Equation (9).

$$T_{snew} = \frac{\Delta t}{mc_p}(Q_{solar} - Q_{Load} - Q_{TankLoss}) + T_{sprevious} \qquad (9)$$

Different models were conducted for different sets of parameters, altering the heat rate from the solar system, the heat rate to the load, and the amount of heat loss from the tanks. Each model uses a starting storage temperature of 90 ^{o}C (@ t=0) and an ambient air temperature of 20 ^{o}C. Figure 18 displays the temperature decay profile for both storage tanks (160 gallons total). The $(UA)_s$ value used was determined experimentally and is 9.0 W/^{o}C.
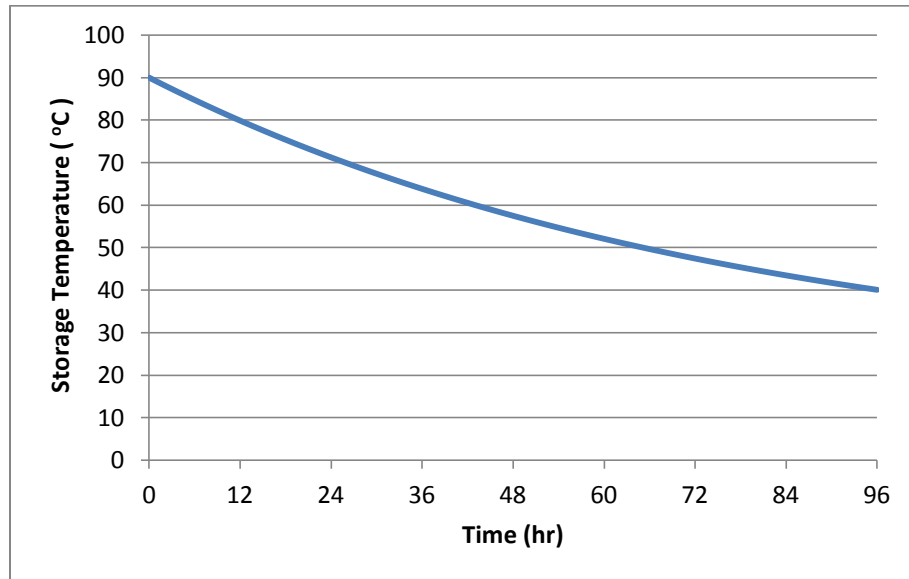
Figure 18: Modeling calculations for the storage tank heat loss.

Figure 19 displays the temperature decay profile of the storage tank with a 4.0 kW load, simulating the load of Application 1 with no incoming solar energy.
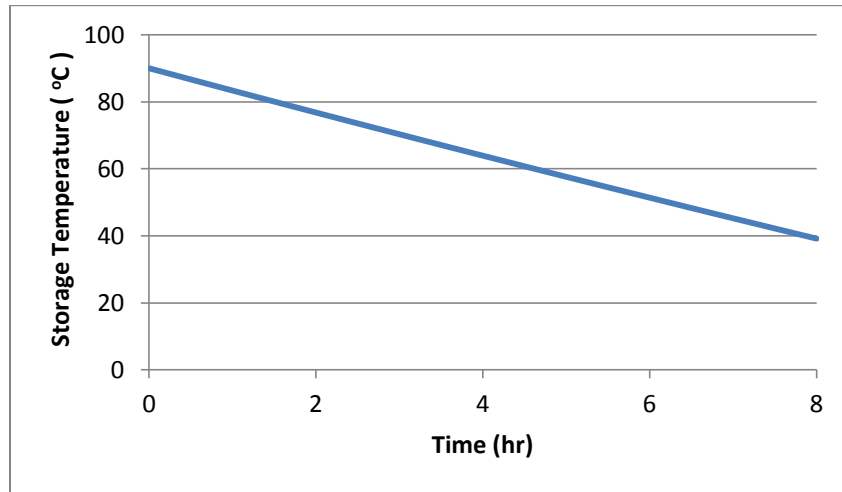
Figure 19: Modeling calculations simulating a 4.0 kW load with no solar energy.

4.7 Application 2: Description of Flat Plate Heat Exchanger

The type of heat exchanger selected for the boiler water preheat system is a counter-flow, flat plate, liquid-liquid heat exchanger. The advantage of plate heat exchangers over conventional coil heat exchangers is that the fluid is exposed to a greater surface area, therefore increasing the amount of heat transferred between the fluids.

The heat exchanger selected for this application was the GEA PHA Systems Brazed Plate Heat Exchanger, model FG3x8-20 [11]. It features a fully brazed construction which allows for high operating pressures as well as a leak-tight construction. The stacked construction of the plates allows for two separate flow passages between the plates, allowing a liquid to flow between every other plate. This allows for complete separation between the two mediums. This can be seen in a schematic of the heat exchanger in Figure 20. Corrugations in each of the plates create high turbulence of the fluids,

resulting in greater heat transfer. The plate material is a 316L Marine Grade Stainless Steel, chosen for its ability to withstand high temperatures and its corrosion resistance. The dimensions of the heat exchanger are displayed in Table VII, which references the dimensions in Figure 20.
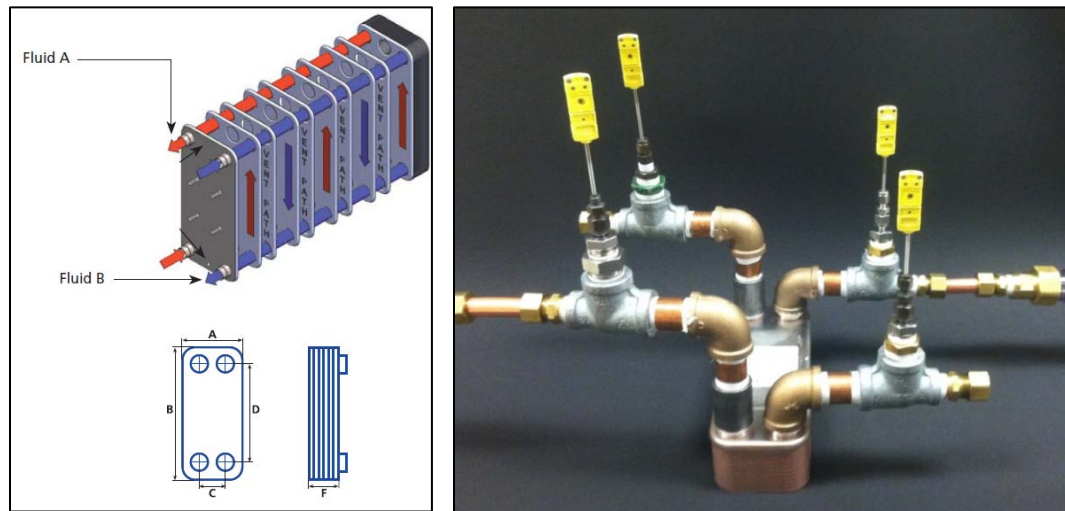
Figure 20: Displays a schematic of the flat plates and fluid separation within the heat exchanger (left). Displays the actual flat plate heat exchanger (right).

Table VII: Displays the dimensions of the flat plate heat exchanger.

Dimensions of Heat Exchanger	
A(mm)	86
B (mm)	226
C (mm)	43
D(mm)	183
F(mm)	55
# plates	20

4.8 Application 2: Heat Exchanger Testing System

In order to test the Flat Plate Heat Exchanger a small scale pumping loop station was constructed in the laboratory. The apparatus was comprised of a two-loop system; the "solar loop", in order to simulate the hot thermal storage loop of the existing system, and the "storage loop", simulating the pre-heat into the water-heater. A schematic of the testing apparatus is displayed in Figure 21.
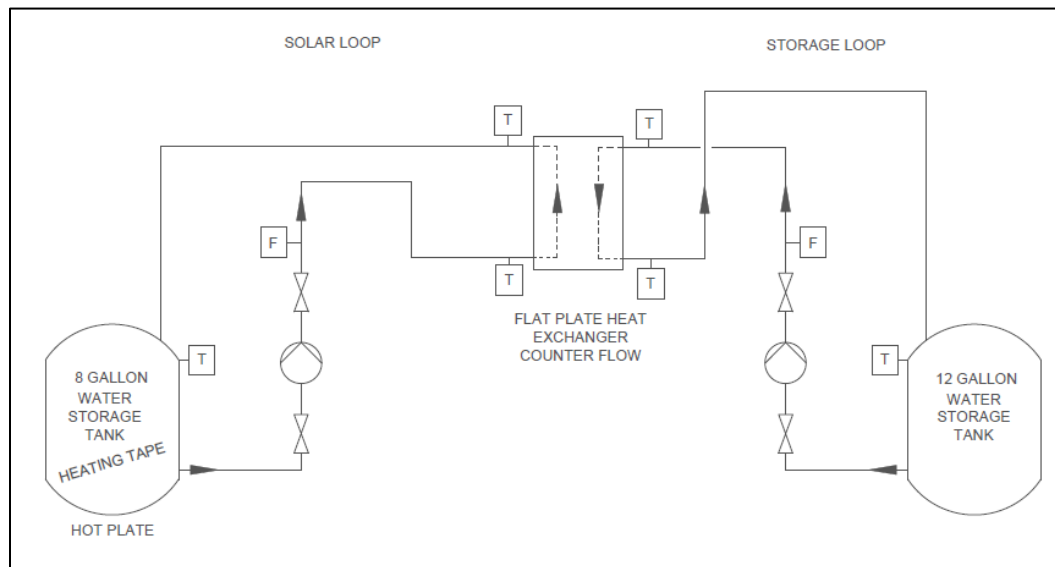
Figure 21: Schematic of the heat exchanger testing apparatus.

The solar loop consisted of a steel, 8-gallon tank which was heated via two types of heating tapes, wrapped around the circumference of the tank, and a hot plate, placed under the tank. Water was pumped from the tank using a 1/25 hp, cast iron, Taco centrifugal pump. The flow rate was measured using a Hedland EZ-VIEW flow meter. After passing through the heat exchanger, the water circulated back to the storage tank.

The storage loop consisted of a 15-gallon steel tank. The same model flow meter and pump were used in this loop. Both loops were constructed using ½" copper tubing. Both

tanks, tubing, and the heat exchanger were wrapped in ½" insulation in order to minimize heat loss. Six thermocouples, type K, were used to measure the water temperatures throughout the system. Four were placed at the inlet and outlets of the heat exchanger while the other two were placed in the tanks. The system apparatus is displayed in Figure 22. A complete Bill of Materials is displayed in Appendix B along with the projects budget in Appendix C.
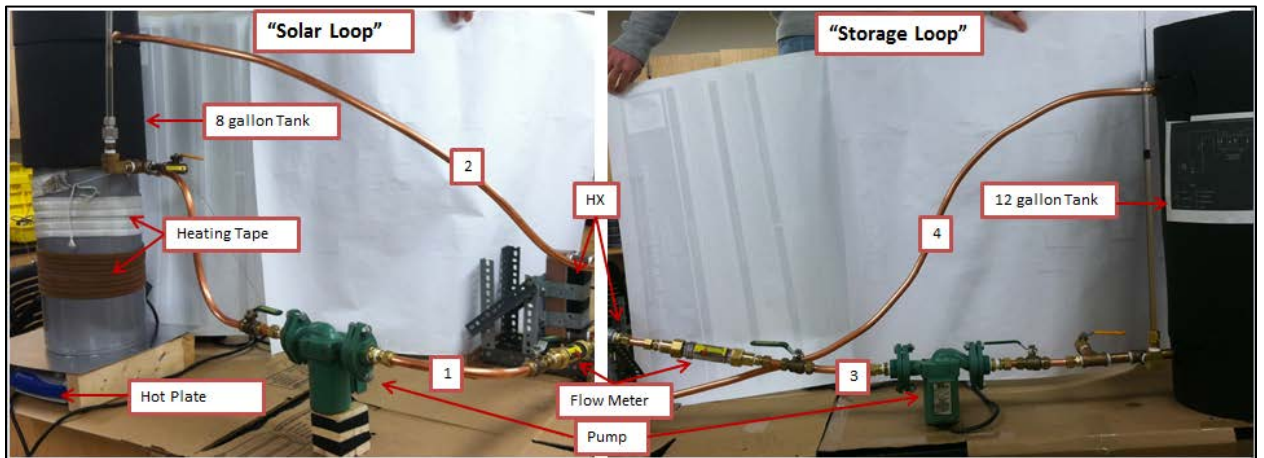
Figure 22: Displays both loops of the testing apparatus. 1) Supply from tank to HX. 2) Return from HX to tank. 3) Supply from tank to HX. 4) Return from HX to tank.

4.9 Application 2: Characterization of Heat Exchanger

The flat plate heat exchanger was first characterized by running multiple system trials and altering the system parameters such as flow rate and starting tank temperature. The following trial had an initial "solar" side tank temperature of 96.6 ^{o}C. At the start of the trial the input heat was turned off and the pumps were turned on. The solar side had a flow rate of 1.5 gpm while the storage side had a flow rate of 1.25 gpm. The inlet and outlet water temperatures of the heat exchanger are displayed in Figure 23.
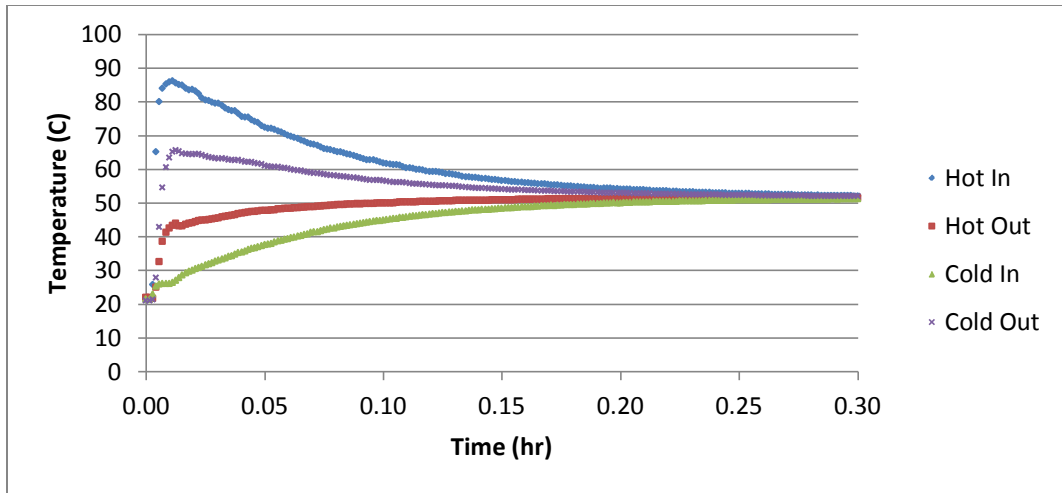
Figure 23: Displays the four temperatures taken at the inlet and outlet states of the heat exchanger.

Figure 24 displays the rate of heat transfer on both sides of the heat exchanger. The difference in the heat rate at any given time is the heat that is lost. Insulation surrounded the heat exchanger to try and minimize this heat loss. The maximum heat rate transferred to the storage loop was 12.6 kW while 16.7 kW was transferred from the solar side. This results in a rate of heat loss of 4.1 kW across the heat exchanger. Over time, the temperatures of both loops converge resulting in no heat being transferred across the heat exchanger. This trend is displayed in Figure 24.
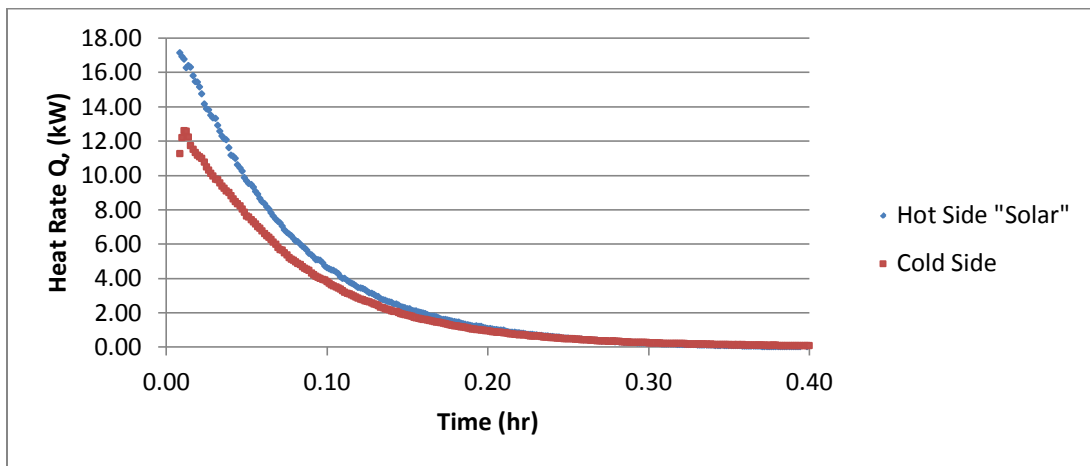
Figure 24: Displays the rate of heat transfer on both sides of the heat exchanger.

According to the manufactures specification, the maximum capacity of the heat exchanger is given to be 29.3 kW (100,000 BTU/hr) [11]. This was not achieved during testing due to the limitations of initial water temperature and the flow rates of the testing system. The maximum limitations given were of 176 ^{o}C and 10 gpm while this trail was only operating at 96 ^{o}C and 1.5 gpm.

A LMTD and an NTU-ε analysis were conducted on the flat plate heat exchanger, as discussed in Section 4.3. Table VIII displays the LMTD results while Table IX displays the NTU-ε results.

Table VIII: Displays the results from the LMTD analysis conducted on the flat plate heat exchanger.

Q (kW)	3.8
LMTD	11.8
UA (W/^{o}C)	**325**

Table IX: Displays the results from the NTU-ε analysis conducted on the flat plate heat exchanger.

effectiveness (ε)	0.69
NTU	4.4
UA (W/^{o}C)	**1427**

Although it is a different size and model, the resulting UA value for the flat plate heat exchanger is similar to that discussed in Section 4.3.

4.10 Application 2: Heat Transfer Analysis of Testing System

An energy balance analysis was performed on the testing apparatus to determine how much heat was being lost throughout the system. First the 8-gallon, solar loop tank was analyzed to determine the efficiency of how much energy was being transferred into the water by the heating elements. Using a Watts Up Electricity Monitor, the amount of electricity being drawn from three elements was measured and is displayed in Table X. The readings were taken over a 235 minutes time span. From this total energy being exerted toward heating was calculated and is also displayed in Table X.

Table X: Displays the amount of energy drawn from the electric heating units.

	Q_{in} (kW)	E_{in} (MJ)
Heating Tape 1, Brisk Heat	0.531	7.5
Heating Tape 2	0.504	7.1
Hot Plate, Fisher Scientific	0.8	11.3
Total	**1.835**	**25.9**

Over this time period the water temperature increased from 22.6 ^{o}C to 96.5 ^{o}C, resulting in a 70.7 ^{o}C temperature differential. Given the 6.6 gallons in the tank, this resulted in a total thermal storage of 7.3 MJ. Thus concluding the method of heating the tanks was only 28% efficient.

The heaters were then turned off, and the pumps were turned on. Once the system approached equilibrium the temperature in the 12 gallon, storage loop tank was measured. The temperature rose from 27.0 ^{o}C to 54.4 ^{o}C for a temperature differential of

23.8 °C. Given the 9.9 gallons in the tank, this resulted in a total thermal storage of 3.8 MJ. Therefore, of the 7.3 MJ originally in the solar loop tank, 52% of the energy was lost in the system. The converging tank temperatures are displayed in Figure 25.
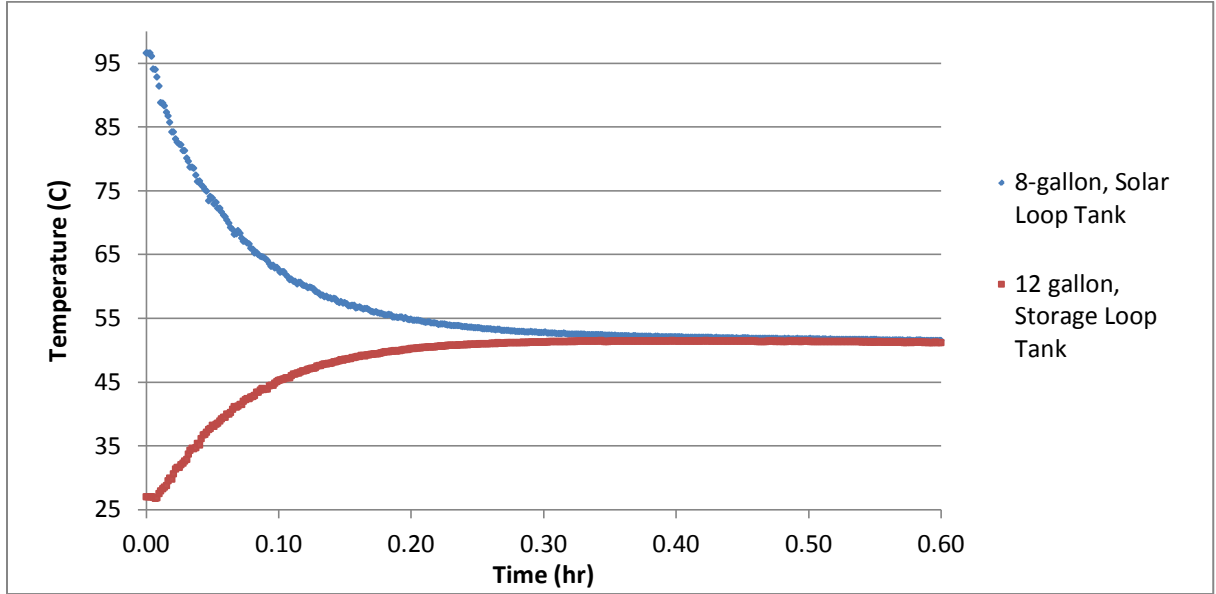
Figure 25: Displayed the converging tank temperatures once the system was turned on.

The heat loss in the 12-gallon, storage loop tank was then analyzed using Equation (8). This can be written as a temperature differential, as expressed in Equation (9)

$$Q_{TankLoss} = mc_p \frac{d\theta_s}{dt} = (UA)_s \theta \qquad (9)$$

In order to determine the overall heat loss coefficient of the storage tank, $(UA)_s$, Equation (9) was first rearranged and integrated (Equation (10)).

$$\int_i \frac{1}{\theta} \frac{d\theta_s}{dt} = \int_i \frac{(UA)_s}{mc_p} \qquad (10)$$

This resulted in a linear expression for the temperature decay of the storage tank in terms of its heat loss parameters (Equation (11)).

$$\ln(\theta) = \frac{(UA)_s}{mc_p} \theta_i + \ln(\theta_i) \qquad (11)$$

33

A trail was conducted with an initial storage tank temperature of 70 $^{\circ}$C. The system was turned off and was the temperature decay was measured. The expression was plotted and is displayed in Figure 26.
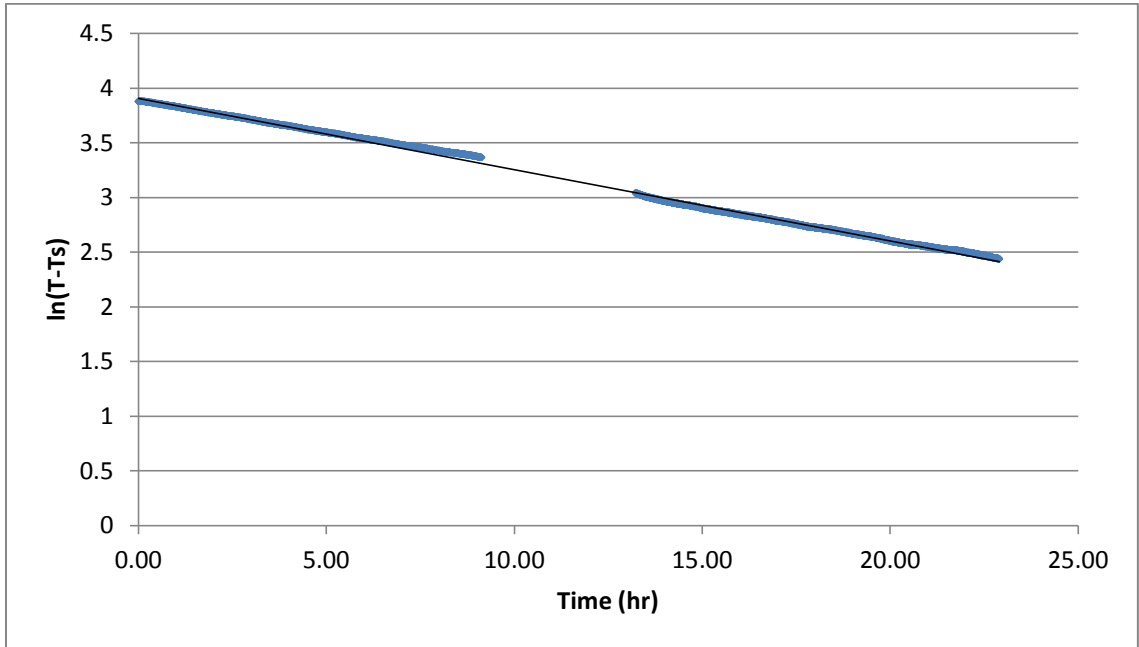
Figure 26: Displays the logarithmic of the temperature decay of the storage tank. Note: The gap in data resulting from a computer malfunction.

By fitting a linear regression line to the plot, the slope of the line, $\frac{(UA)_S}{mc_p}$, was determined. The overall heat transfer coefficient-surface area product was then determined to be 10.1 W/$^{\circ}$C.

4.11 Application 2: Fluid Mechanic Analysis of Testing System

A fluid mechanic analysis was conducted on the testing system to determine the total head loss around each loop. The modified Bernoulli's equation, displayed in Equation (12), was used to calculate the head loss of the system.

$$\frac{p_1}{\rho g} + \frac{V_1^2}{2g} + z_1 = \frac{p_2}{\rho g} + \frac{V_2^2}{2g} + z_2 + \left[\frac{fL}{D_h} + \sum K\right]\frac{V^2}{2g} \qquad (12)$$

The kinetic and potential energy terms of Equation (12) are assumed to have values of zero, resulting in Equation (13), an unknown pressure difference equal to the minor and major losses of the system.

$$\frac{p_1 - p_2}{\rho g} = \left[\frac{fL}{D_h} + \sum K\right]\frac{V^2}{2g} \qquad (13)$$

The pressure drop through the heat exchanger was included by the additional term, Δp. This value was given by the manufactures specifications.

$$\frac{p_1 - p_2}{\rho g} = \left[\frac{fL}{D_h} + \sum K\right]\frac{V^2}{2g} + \frac{\Delta p}{\rho g} \qquad (14)$$

The values used as well as the corresponding head loss in each loop are displayed in Table XI.

Table XI: Displays the head loss calculations for each loop of the testing system.

Variables	Solar Loop	Storage Loop
D, Pipe Diameter (m)	0.01	0.01
f, (roughness)	0.000002	0.000002
ΣK, Resistance Coefficient	25.3	22.3
V, Velocity (m/s)	1.37	1.37
Head, Heat Exchanger (m)[13]	0.28	0.28
Total Head Loss	2.70	2.70

The calculated values were compared with the manufactures pump curve, (Figure 27) which predicts a head loss of approximately 2.8 meters at the 2.75 gpm flow rate which was observed in both loops of the system.
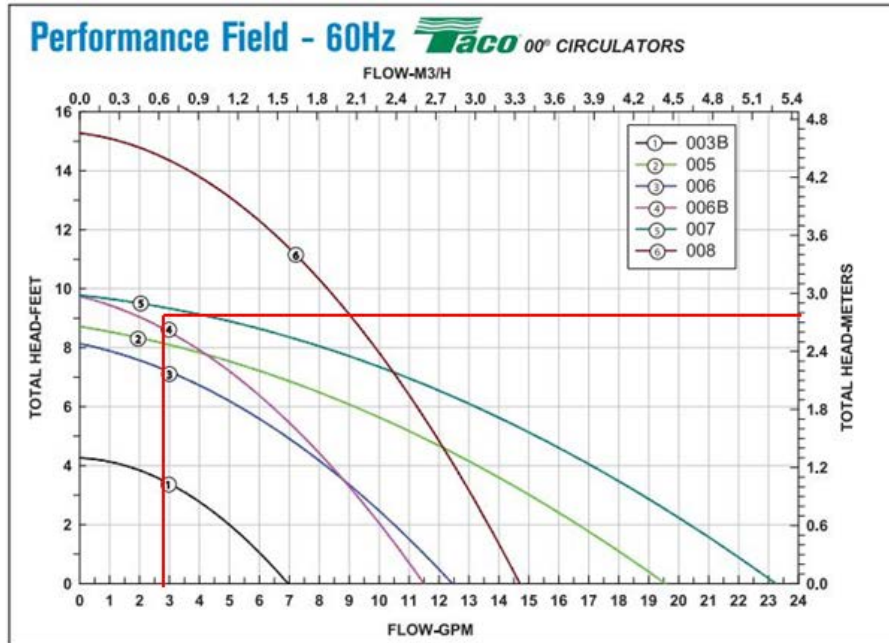
Figure 27: Displays the pump curve for the 1/25 hp Taco Pump. Curve number 5 on the figure corresponds to the 007 model used in the testing system. [13]

5. Conclusion and Summary

This project has involved the analysis, design, and testing of potential applications for Union College's liquid-based solar thermal collector system. The existing system features nine, 16-tube, evacuated tube solar modules. Through a two loop non-mixing system, thermal energy is stored in water within two-80 gallon storage tanks. It has been proven through previous research that this system was shown to produce thermal energy at a rate of 13 kW and a total daily thermal output of 80 MJ. Two potential applications were researched in order to provide a use for this thermal energy. These applications include: Application 1: Liquid-Air Heat Exchanger, and Application 2: Boiler Water Preheat System.

The liquid-air heat exchanger in Application 1 was determined to be a cross-flow, mixed-unmixed heat exchanger. It was shown to provide thermal energy at a rate of 4.0 kW and supply air at 40 ^{o}C to a given space under the testing conditions. The total power required by the fans on the heat exchanger was only 72 W. The overall heat transfer coefficient-surface area product (*UA*) was calculated to be 571 W/^{o}C. The implementation of this application seems to be a plausible application for the solar thermal system.

In the study conducted to measure the water consumption of the Facilities Building, it was determined that the installation of Application 2 may not be worthwhile to pursue for this specific location. Over a 12 week time period, the building only consumed 8.638 gallons of hot water. Due to the amount of heat that the solar thermal system produces, this application would only utilize a small portion of that heat which would not be worth

the equipment and running costs of this application. The prediction of increased water consumption due to the falling winter temperatures was shown to be incorrect.

Although this system would not be a worthwhile investment in the Faculties Building, it does prove to be a worthwhile technology. The small scale pumping station constructing in the laboratory demonstrated the functionality of a flat plate heat exchanger that would suit the needs of this application. A characterization of this heat exchanger yielded similar results to the existing flat plate in the existing system.

No construction on either of the applications was started due the solar systems lack of functionality over these few winter months. The glycol and water mixture was never added to the system at the start of winter, and was therefore not able to be run. With the approval of the Cogeneration System that will be installed in the Facilities Building, the solar system will unfortunately have to be dismantled or relocated due to construction. The research and equipment purchased for this project will fortunately be available for the future use of the system, wherever that may be.

6. References

[1]"Overview of Greenhouse Gases." 9 September 2013. *EPA*. September 2013.

[2] News, National Geographic. "Global Warming Fast Facts." 14 June 2007. *National Geographic*. September 2013.

[3] NYSERDA. *NYSERDA.gov*. 2013. September 2013.

[4] Wilk, Richard D. *Development of a High Perfomance-Optically Enhanced Solar Thermal Collector System to Power a Trochoidal Gear Engine/Generator*. Report. Schenectady, NY, 2012.

[5] "SundogSmartHouse." *Sundog Solar*. N.p., n.d. Web. 11 Nov. 2013.

[6] "How Does a Solar Thermal Flat Plate Collector Work?" *Go Green Heat Solutions*. International Technolody Sourcing: Solar Division, n.d. Web. 16 Nov. 2013.

[7] "Evacuated Tube Solar Collectors vs. Flat Plate Solar Collector." *SolarPlusGreen*. N.p., n.d. Web. 16 Nov. 2013.

[8] Bergman, T. L. *Introduction to Heat Transfer*. Hoboken, NJ: John Wiley & Sons, 2011.
Print.

[9] "7112 N: DC Axial Compact Fan." *Ebmpapst*. N.p., n.d. Web. 15 Nov. 2013.

[10] "Space Saving Heat Exchanger." *McMaster-Carr*. N.p., n.d. Web. 15 Nov. 2013.

[11] "Welcome to the World of Plate Heat Exchangers." *GEA PHE Systems*. N.p., n.d. Web. 11 Feb. 2014.

[12] "Taco-HVAC: Water Circulation Pumps & Circulators." *Taco-HVAC*. N.p., n.d. Web. 9 Mar. 2014.

[13] "Weather History for Schenectady, NY." *WunderGround*. N.p., 14 Nov. 2013. Web. 15 Nov. 2013.

7. Appendix

7.1 Appendix A: Water Consumption and Temperature Data

	Cumulative Usage (gallons)	Weekly Usage	% Weekly	Average Weekly Temperature (^{o}C) [13]
3-Oct	0	0	0	
10-Oct	0.418	0.418	5	14
17-Oct	0.977	0.559	6	13
24-Oct	1.49	0.513	6	12
31-Oct	1.789	0.299	3	6
7-Nov	2.256	0.467	5	8
14-Nov	2.685	0.429	5	3
21-Nov	2.999	0.314	4	7
28-Nov	3.336	0.337	4	-2
5-Dec	3.685	0.349	4	-1
12-Dec	4.076	0.391	5	1
19-Dec				-7
26-Dec				-1
2-Jan	5.097	1.021		-4
9-Jan	5.492	0.395	5	-13
16-Jan	5.778	0.286	3	2
23-Jan	6.183	0.405	5	-5
30-Jan	6.637	0.454	5	-12
6-Feb	6.997	0.36	4	-4
13-Feb	7.229	0.232	3	-9
20-Feb	7.587	0.358	4	-5
27-Feb	7.946	0.359	4	-1
6-Mar	8.179	0.233	3	-8
13-Mar	8.638	0.459	5	-2

7.2 Appendix B: Testing System: Bill of Material

Bill of Materials- Testing Apparatus		
Item	**Size Description**	**Qty.**
HX	20 Plate,3/4" thread, (3"x8")	1
Pump	1/25 HP, Taco Cast Iron	2
Tank	12 Gal	1
Tank	8 gal	1
Flow Meters	Versa Mount- '1/2 female	2
Copper Tubing	1/2"- 6ft	3
Type K Thermo.	(1/8" SS, 6")	4
Type K Thermo.	(1/8" SS, 12")	2
Thermo. Fitting	Female Caps	6
Thermocouple Wire		
Lever-Ball Valve	1/2" comp. fittings	4
Lever Ball Valve	1/2" female	2
Pipe-Comp. Fitting	1/2" pipe to tube	16
Tee (HX)	3/4/"-3/4"-1/2" female	4
Tee (Tank Supply)	1/2" female-female-male	2
Tee	1/2" Female	5
Nipple	1/2"	6
Nipple	3/4" Brass	6
90 Elbo	3/4" Brass	2
Couplings	3/4" Black Steel	2
Bushing	3/4" pipe to 1/2" pipe	8
Bushing	1/2" Male pipe- 1/4" Tube	5
Bushing	1/4" Comp- 1/8" Comp	6

7.3 Appendix C: Testing System: Budget

GREEN GRANT-Bill of Materials					Budget			
Item	Size Despription	Manufacturer and Model Number	Supplier	Qty.	Price per Unit ($)	Total Price	Date of Purchase	Balance
								$1,504.00
HX	20 Plate,3/4" thread, (3"x8")		Pex Supply	1	$229.42	$ 229.42	1 Nov. 2013	$1,274.58
Copper Tubing	1/2- 6ft	8967K69	McMaster	3	$ 35.12	$ 105.36		$1,169.22
Tank	8 gal	3667K1	McMaster	1	$ 92.47	$ 92.47		$1,076.75
Flow Meters	1/2 female	4197K21	McMaster	2	$104.21	$ 208.42		$ 868.33
Couplings	3/4"	46685K265	McMaster	2	$ 3.27	$ 6.54	7 Feb. 2014	$ 861.79
Nipple	3/4"	4568K191	McMaster	6	$ 3.32	$ 19.92	7 Feb. 2014	$ 841.87
90 Elbo	3/4"	4429K164	McMaster	2	$ 9.07	$ 18.14	7 Feb. 2014	$ 823.73
Pipe-Comp. Fitting	1/2 pipe to tube	50915K332	McMaster	4	$ 7.04	$ 28.16	25 Feb. 2014	$ 795.57
Bushing	3/4 pipe to 1/2 pipe	4429K414	McMaster	4	$ 4.40	$ 17.60	25 Feb. 2014	$ 777.97
Lever Ball Valve	1/2" female	47865K23	McMaster	2	$ 9.47	$ 18.94	27 Feb. 2014	$ 759.03
Notes:								
1) Does not include Shipping fees.								
STUDENT RESEACH GRANT- Bill of Materaials					Budget			
Item	Size Despription	Manufacturer and Model Number	Supplier	Qty.	Price per Unit ($)	Total Price	Date of Purchase	Balance
								$ 411.00
Tee (HX)	3/4-3/4-1/2 female	4638K189	McMaster	4	$ 7.22	$ 28.88	29 Jan. 2014	$ 382.12
Pipe-Comp. Fitting	1/2 pipe to tube	50915K332	McMaster	12	$ 7.04	$ 84.48	29 Jan. 2014	$ 297.64
Tee (Tank Supply)	1/2 female-female-male	4429K326	McMaster	2	$ 21.80	$ 43.60	29 Jan. 2014	$ 254.04
Lever-Ball Valve	1/2 comp. fittings	4067T21	McMaster	4	$ 10.07	$ 40.28	29 Jan. 2014	$ 213.76
Shipping				1	6.56	$ 6.56	29 Jan. 2014	$ 207.20
Type K Thermo.	(1/8" SS, 6")	KMQSS-125U-6	Omega	4	$ 29.00	$ 116.00	31 Jan. 2014	$ 91.20
Type K Thermo.	(1/8" SS, 12")	KMQSS-125U-12	Omega	2	$ 30.00	$ 60.00	31 Jan. 2014	$ 31.20
Thermo. Fitting		SMPW-K-F	Omega	6	$ 2.40	$ 14.40	31 Jan. 2014	$ 16.80
Shipping				1	$ 10.00	$ 10.00	31 Jan. 2014	$ 6.80
Notes:								
1) SRG Credit Card has been returned: 3 Feb. 2014								

7.4 Appendix D: Fluid Mechanic Analysis

Fittings	K	Solar Loop		Storage Loop	
		Amount	ΣK	Amount	ΣK
Ball Valve	0.08	2	0.16	2	0.16
90° Elbo	0.75	2	1.5	2	1.5
Tee (through)	0.54	1	0.54	4	2.16
Tee (around)	1.62	2	3.24	0	0
Flow Meter	15	1	15	1	15
Tube Fitting	0.15	8	1.2	8	1.2
Bushing	0.2	2	0.4	0	0
Nipple	0.07	4	0.28	4	0.28
Thermo. Fittings	1	3	3	2	2
ΣK			25.3		22.3
Head Loss (m)			2.41		2.41
Heat Exchanger Head loss(m)			0.28		0.28
Total Head Loss (m)			**2.70**		**2.70**